







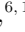




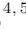




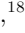



Statistical association between the candidate repeating FRB 20200320A and a galaxy group

MASOUD RAFIEI-RAVANDI ^{1,2} KENDRICK M. SMITH ³ D. MICHILLI ^{4,5} ZIGGY PLEUNIS ⁶ MOHIT BHARDWAJ ⁷
MATT DOBBS ^{1,2} GWENDOLYN M. EADIE ^{6,8} EMMANUEL FONSECA ^{9,10} B. M. GAENSLER ^{6,11,12}
JANE KACZMAREK ^{13,14} VICTORIA M. KASPI ^{1,2} CALVIN LEUNG ¹⁵ DONGZI LI ¹⁶ KIYOSHI W. MASUI ^{4,5}
AYUSH PANDHI ^{11,6} AARON B. PEARLMAN ^{1,2} EMILY PETROFF ³ MUBDI RAHMAN ¹⁷ PAUL SCHOLZ ^{18,6} AND
DAVID C. STENNING ¹⁹

¹*Department of Physics, McGill University, 3600 rue University, Montréal, QC H3A 2T8, Canada*

²*Trottier Space Institute, McGill University, 3550 rue University, Montréal, QC H3A 2A7, Canada*

³*Perimeter Institute for Theoretical Physics, 31 Caroline Street N, Waterloo, ON N2S 2YL, Canada*

⁴*MIT Kavli Institute for Astrophysics and Space Research, Massachusetts Institute of Technology, 77 Massachusetts Ave, Cambridge, MA 02139, USA*

⁵*Department of Physics, Massachusetts Institute of Technology, 77 Massachusetts Ave, Cambridge, MA 02139, USA*

⁶*Dunlap Institute for Astronomy & Astrophysics, University of Toronto, 50 St. George Street, Toronto, ON M5S 3H4, Canada*

⁷*Department of Physics, Carnegie Mellon University, 5000 Forbes Avenue, Pittsburgh, 15213, PA, USA*

⁸*Department of Statistical Sciences, University of Toronto, 700 University Ave., Toronto, ON M5G 1Z5, Canada*

⁹*Department of Physics and Astronomy, West Virginia University, P.O. Box 6315, Morgantown, WV 26506, USA*

¹⁰*Center for Gravitational Waves and Cosmology, West Virginia University, Chestnut Ridge Research Building, Morgantown, WV 26505, USA*

¹¹*David A. Dunlap Department of Astronomy & Astrophysics, University of Toronto, 50 St. George Street, Toronto, ON M5S 3H4, Canada*

¹²*Division of Physical and Biological Sciences, University of California Santa Cruz, Santa Cruz, CA 95064, USA*

¹³*CSIRO Space & Astronomy, Parkes Observatory, P.O. Box 276, Parkes NSW 2870, Australia*

¹⁴*Department of Computer Science, Math, Physics, & Statistics, University of British Columbia, Kelowna, BC V1V 1V7, Canada*

¹⁵*Department of Astronomy, University of California Berkeley, Berkeley, CA 94720, USA*

¹⁶*Cahill Center for Astronomy and Astrophysics, MC 249-17 California Institute of Technology, Pasadena CA 91125, USA*

¹⁷*Sidrat Research, 124 Merton Street, Toronto, ON M4S 2Z2, Canada*

¹⁸*Department of Physics and Astronomy, York University, 4700 Keele Street, Toronto, ON M3J 1P3, Canada*

¹⁹*Department of Statistics & Actuarial Science, Simon Fraser University, 8888 University Dr, Burnaby, BC V5A 1S6, Canada*

ABSTRACT

We present results from angular cross-correlations between select samples of CHIME/FRB repeaters and galaxies in three photometric galaxy surveys, which have shown correlations with the first CHIME/FRB catalog containing repeating and nonrepeating sources: WISE×SCOS, DESI-BGS, and DESI-LRG. We find a statistically significant correlation (p -value < 0.001 , after accounting for look-elsewhere factors) between a sample of repeaters with extragalactic dispersion measure (DM) $> 395 \text{ pc cm}^{-3}$ and WISE×SCOS galaxies with redshift $z > 0.275$. We demonstrate that the correlation arises surprisingly because of a statistical association between FRB 20200320A (extragalactic DM $\approx 550 \text{ pc cm}^{-3}$) and a galaxy group in the same dark matter halo at redshift $z \approx 0.32$. We estimate that the host halo, along with an intervening halo at redshift $z \approx 0.12$, accounts for at least $\sim 30\%$ of the extragalactic DM. Our results strongly motivate incorporating galaxy group and cluster catalogs into direct host association pipelines for FRBs with $\lesssim 1'$ localization precision, effectively utilizing the two-point information to constrain FRB properties such as their redshift and DM distributions. In addition, we find marginal evidence for a negative correlation at 99.4% CL between a sample of repeating FRBs with baseband data (median extragalactic DM = 354 pc cm^{-3}) and DESI-LRG galaxies with redshift $0.3 \leq z < 0.45$, suggesting that the repeaters might be more prone than apparent nonrepeaters

to propagation effects in FRB-galaxy correlations due to intervening free electrons over angular scales $\sim 0.5^\circ$.

Keywords: Cosmology (343); High energy astrophysics (739); Large-scale structure of the universe (902); Radio transient sources (2008)

1. INTRODUCTION

One of the most rapidly evolving fields of astrophysics is the study of extragalactic fast radio bursts (FRBs). FRBs are highly energetic ($\sim 10^{36-42}$ erg) flashes of radio waves of unknown origins (for a recent review, see Petroff et al. 2022). In contrast to their intrinsic pulse widths that last for \sim milliseconds, the FRB arrival time at Earth can be delayed, e.g., from \sim seconds to \sim minutes across the 400–800 MHz band, proportional to ν^{-2} , where ν is the observed frequency. This dispersion is a result of the interaction between propagating radio waves and intervening free electrons from the source to observer. In the dispersion relation, the constant of proportionality is defined as the dispersion measure $DM \equiv \int n_e dx$, where x is the distance and n_e is the free electron column density along the line of sight, broadly accounting for contributions from the FRB host (DM_{host}), intergalactic medium (DM_{IGM}), and Milky Way (DM_{gal}) as well as other structures (e.g., intervening galaxy groups and clusters).

The first FRB was unearthed serendipitously from archival data dating back to 2001 (Lorimer et al. 2007). Since then, radio telescopes such as the Canadian Hydrogen Intensity Mapping Experiment (CHIME; CHIME Collaboration 2022) have dedicated a large fraction of their computational and human resources to detecting and analyzing these mysterious signals. At the time of writing, about 40 FRBs had been localized to their host galaxies (see, e.g., Chatterjee et al. 2017; Bannister et al. 2019; Ravi et al. 2019; Bhandari et al. 2020; Heintz et al. 2020; Law et al. 2020; Macquart et al. 2020; Marcote et al. 2020; Bhardwaj et al. 2021a; Bhandari et al. 2022, 2023; Gordon et al. 2023; Law et al. 2023; Michilli et al. 2023; Sharma et al. 2023). FRB host associations are usually carried out through cross-matching coordinates of single galaxies with FRBs. However, depending on galaxy survey completeness limits, galaxy redshifts, FRB localization uncertainty, and DM, an FRB may be found to be plausibly associated with just one or many galaxies (for a review on direct host associations, see Eftekhari & Berger 2017). Enabled through its large field of view (~ 200 sq. deg.), wide bandwidth (400–800 MHz), and highly optimized software, the CHIME Fast Radio Burst instrument (CHIME/FRB; CHIME/FRB Collaboration 2018) detects a few FRBs per day, which over

the production period of a few years ($\mathcal{O}(10^3)$ FRBs) has resulted in a wide range of FRB population studies. CHIME/FRB sources have localization uncertainties of $\sim 10'$ (real-time intensity beams) or $\lesssim 1'$ (through saved voltage data) that are generally not sufficient for per-object analyses such as cross-matching FRBs with auxiliary catalogs of, e.g., spectroscopic redshift galaxies or X-ray sources (for an exception, see Bhardwaj et al. 2021b, in which a CHIME/FRB source was localized robustly to the outskirts of M81). Thus far, CHIME/FRB population studies have relied on the large number of sources with localization uncertainties of $\sim 10'$. For instance, Josephy et al. (2021) showed that CHIME/FRB Catalog 1 (CHIME/FRB Collaboration 2021) does not correlate spatially with the Galactic plane. To date, $\sim 3\%$ of CHIME/FRB sources have emitted repeating bursts sporadically or periodically over long time intervals of \sim days–months (CHIME/FRB Collaboration 2023). Compared to apparent nonrepeaters (hereafter, for brevity, nonrepeaters), repeaters exhibit wider pulse widths and narrower bandwidths (Pleunis et al. 2021). Using the observed DM distributions, CHIME/FRB Collaboration (2023) showed that the repeating and nonrepeating FRB populations differ statistically at $\approx 2.5-3\sigma$ levels. In this work, we compare the two populations through their angular cross-correlations with photometric redshift catalogs of galaxies (for a comprehensive formalism of FRB-galaxy correlations, see Rafiei-Ravandi et al. 2020).

This is a follow-up analysis based on Rafiei-Ravandi et al. (2021), who reported statistically significant (p -values $\sim 10^{-4}$) correlations between unique FRB sources (i.e., single bursts for repeaters as well as nonrepeaters) in CHIME/FRB Catalog 1 (median extragalactic $DM \approx 536 \text{ pc cm}^{-3}$) and galaxies in the WISE \times SCOS, DESI-BGS, and DESI-LRG surveys. Rafiei-Ravandi et al. (2021) showed that the strength and angular scale of FRB-galaxy correlations are consistent with an order-one fraction of the Catalog 1 FRBs inhabiting the same dark matter halos that host galaxies in the redshift range $0.3 \lesssim z \lesssim 0.5$. In addition, Rafiei-Ravandi et al. (2021) found statistical evidence for a subpopulation of FRBs with high DM_{host} ($\sim 400 \text{ pc cm}^{-3}$), and showed that this could be explained through the host halo DM (DM_{hh}) contribution for FRBs near the centers of massive ($\sim 10^{14} M_\odot$) halos.

In this work, we present results from the FRB-galaxy correlation analysis for a sample of 25 newly cataloged repeaters and 14 candidate repeating FRB sources (CHIME/FRB Collaboration 2023) along with 18 previously published repeaters (CHIME/FRB Collaboration 2019a,b; Fonseca et al. 2020; Michilli et al. 2023), 41 of which have baseband localizations. The CHIME/FRB baseband pipeline (Michilli et al. 2021) records raw voltage data that allow for sky localizations $\lesssim 1'$, enabling cross-correlation studies at high multipoles $\ell \sim 10^4$, where a large number of harmonic modes can give rise to a large signal-to-noise ratio from two-point correlations between FRBs and galaxies in the same dark matter halos, i.e., the one-halo term in the FRB-galaxy cross power spectrum (see, e.g., Figures 2 and 8 in Rafiei-Ravandi et al. 2021, 2020, respectively).

Statistical cross-correlations between FRB and galaxy catalogs have significant constraining power over a wide range of spatial scales, including the two-halo, one-halo, and Poisson terms (see Rafiei-Ravandi et al. 2020). For FRB catalogs with sub-arcsec localization precision, the two-point information is fully recovered in direct host associations, which attempt to trace FRBs back to their origins in single galaxies. In this work, we present an exceptional example that demonstrates how direct associations with catalogs of galaxy groups or clusters can still recover information for constraining, e.g., an FRB redshift in the absence of an exactly identified host galaxy. FRB-galaxy group/cluster associations have been proposed in a few recent works. For example, Connor & Ravi (2022) cross-matched CHIME/FRB Catalog 1 with a galaxy group catalog (Kourkchi & Tully 2017) in order to place modest constraints on the baryonic content of the circumgalactic medium (CGM) in the local Universe (< 40 Mpc). More recently, Connor et al. (2023) identified two FRB hosts using the DESI group/cluster catalog from Yang et al. (2021). At the time of writing, there had not been any published report on directly cross-matching catalogs of galaxy groups or clusters with roughly localized FRBs that have no associated host galaxies (e.g., a large fraction of CHIME/FRB sources) in order to probe FRB-galaxy associations on one-halo scales and hence place constraints on FRB properties such as their redshift distribution.

We have organized this article as follows. In Section 2, we describe the input catalogs for our cross-correlation pipeline, which is summarized in Section 3. Then, we tabulate and discuss the results in Sections 4 and 5, respectively. Unless specified otherwise, all DM values are extragalactic; we subtract DM_{gal} using the YMW16 (Yao et al. 2017) model throughout. Following Rafiei-Ravandi et al. (2021), we ignore the Milky Way

halo ($29 \lesssim DM_{\text{halo}} \lesssim 111$ pc cm $^{-3}$, Cook et al. 2023; Ravi et al. 2023). Our results are not sensitive to these model assumptions. We adopt a flat Λ CDM cosmology with a Hubble expansion rate $h = 0.67$, matter abundance $\Omega_m = 0.315$, baryon abundance $\Omega_b = 0.048$, initial power spectrum amplitude $A_s = 2.10 \times 10^{-9}$, spectral index $n_s = 0.965$, neutrino mass $\sum_\nu m_\nu = 0.06$ eV, and cosmic microwave background (CMB) temperature $T_{\text{CMB}} = 2.726$ K, which are identical to the assumptions of Rafiei-Ravandi et al. (2021), and consistent with the Planck results of Aghanim et al. (2020).

2. DATA

In this work, we define three FRB samples based on CHIME/FRB Catalog 1 and published repeaters¹ with different localization precisions:

1. *Nonrepeaters*: our first sample contains 457 unique sources, which includes all the apparently non-repeating FRB sources from CHIME/FRB Catalog 1 (CHIME/FRB Collaboration 2021). Following Rafiei-Ravandi et al. (2021), we exclude the sidelobe FRB events 20190210D, 20190125B, and 20190202B. The sample of 457 was localized through real-time intensity beamforming (also known as header localization), which has, on average, a localization error of $\theta_f \sim 10'$.²
2. *Repeaters (baseband)*: 41 CHIME/FRB repeating sources with published baseband localizations (CHIME/FRB Collaboration 2019a,b; Fonseca et al. 2020; Michilli et al. 2023; CHIME/FRB Collaboration 2023). CHIME/FRB baseband localizations result in, on average, localization errors of $\theta_f \lesssim 1'$.
3. *Repeaters (all)*: 52 sources, comprised of the “repeaters (baseband)” sample mentioned above and 11 recently published repeating sources (CHIME/FRB Collaboration 2023). The positions of the latter were obtained by combining multiple header localizations ($\theta_f \sim 1'$).³

Panels (a)–(c) of Figure 1 show the DM distribution for the three samples with median DM values

¹ CHIME/FRB data products are available at <http://www.chime-frb.ca/>.

² The CHIME/FRB beam transfer function can be approximated by a Gaussian with a FWHM θ_f , which is defined as the FRB localization error throughout (Rafiei-Ravandi et al. 2021).

³ Header localizations have confidence regions that can span over multiple disjoint islands (see, e.g., Figure 4 of CHIME/FRB Collaboration (2023)).

497 (a), 354 (b), and 372 (c) pc cm^{-3} , respectively. CHIME/FRB Collaboration (2023) defined two distinct samples of repeaters based on the false positive rate of FRB detections: 25 new repeaters (the “gold” sample) and 14 candidate repeating sources (the “silver” sample). Because of the relatively small total number of repeating sources (compared to nonrepeaters), we combine and use both samples along with other published repeaters throughout this cross-correlation analysis. In addition, we simulate mock FRB catalogs independently for each FRB sample listed above. Mock FRB catalogs have randomized right ascensions, but the same total number of FRBs (N_{FRB}) and other parameters, e.g., declinations, as in the real samples.

For galaxies, we select the three galaxy surveys WISE×SCOS (Bilicki et al. 2016; Krakowski et al. 2016), DESI-BGS, and DESI-LRG (Zhou et al. 2020a), which correlate significantly with CHIME/FRB Catalog 1 (Rafiei-Ravandi et al. 2021). We adopt exactly the same galaxy selection cuts (Krakowski et al. 2016; Ruiz-Macias et al. 2020; Zhou et al. 2020b) and sky masks as adopted by Rafiei-Ravandi et al. (2021). In Table 1, we summarize the relevant properties of these surveys after applying the selection cuts. We note that only a fraction of the FRB samples are unmasked by the galaxy survey footprints (see, e.g., the dashed lines in panels (a)–(c) of Figure 1; the median DM values of nonrepeaters and repeaters (all) change to 538 and 395 pc cm^{-3} after accounting for the WISE×SCOS survey footprint, respectively). Panel (d) of Figure 1 shows the redshift distributions of these galaxy surveys ($z \sim 0.5$), which are desirable for probing statistical correlations with the CHIME/FRB samples (extragalactic DM $\sim 500 \text{ pc cm}^{-3}$).

3. PIPELINE OVERVIEW

Our cross-correlation pipeline is described by Rafiei-Ravandi et al. (2021). Using the same framework (Rafiei-Ravandi 2023),⁴ we generate high-resolution HEALPix (Górski et al. 2005) overdensity maps ($N_{\text{side}} = 8192$) from the FRB (f) and galaxy (g) samples (see Figure 2 here and Figure 3 of Rafiei-Ravandi et al. 2021, respectively). Then, we estimate the amplitude of the angular cross power spectrum C_{ℓ}^{fg} , as a function of multipole (angular wavenumber) ℓ , to a maximum multipole of $\ell_{\text{max}} = 14000$. We assume that the power spectrum for the one-halo term follows a template

Survey	WISE×SCOS	DESI-BGS	DESI-LRG
f_{sky}	0.638	0.118	0.118
$[z_{\text{min}}, z_{\text{max}}]$	[0.0, 0.5]	[0.05, 0.4]	[0.3, 1.0]
z_{med}	0.16	0.22	0.69
N_{gal}	6,931,441	5,304,153	2,331,043
N_{FRB}			
Nonrepeaters	292	168	168
Repeaters (baseband)	26	18	18
Repeaters (all)	35	22	22
Catalog 1	310	183	183

Table 1. Galaxy survey parameters: sky fraction f_{sky} (not accounting for CHIME/FRB coverage; see Rafiei-Ravandi et al. 2021), redshift range $[z_{\text{min}}, z_{\text{max}}]$, median redshift z_{med} , total number of unmasked galaxies N_{gal} , and total number of FRBs N_{FRB} for different samples overlapping the survey.

of the form $C_{\ell}^{fg(1h)} = \alpha e^{-\ell^2/L^2}$, where the amplitude α (a free parameter) captures the one-halo term while the varying template scale L controls the high- ℓ suppression, owing to the CHIME/FRB beam transfer function and FRB-galaxy displacements in the same dark matter halos.

Under the null hypothesis, the total one-halo term would be zero. We estimate the statistical significance of a positive correlation (alternate hypothesis) by computing the maximum of local signal-to-noise ratios $\text{SNR}_{L,z} = \hat{\alpha}_{L,z}/\text{Var}(\hat{\alpha}_{L,z})^{1/2}$ over the 2D parameter space of template scales (L) and redshift endpoints (z) for the data and 1000 mock FRB catalogs.⁵ Finally, we compute a global p -value based on the fraction of mocks with the maximum local significance greater than or equal to the maximum local significance of data: $\max_{L,z}^{(\text{mock})} \text{SNR}_{L,z} \geq \max_{L,z}^{(\text{data})} \text{SNR}_{L,z}$. This procedure fully accounts for the look-elsewhere effect that may arise because of our specific choices in the search space (L, z). In this work, we also discuss the statistical significance of a negative correlation (alternate hypothesis), which is computed through the same procedure as described above, except that we replace all “max” operations with “min”. Subsequently, the global p -value of a negative correlation is reported as the fraction of mocks with the minimum local significance $\min_{L,z}^{(\text{mock})} \text{SNR}_{L,z} \leq \min_{L,z}^{(\text{data})} \text{SNR}_{L,z}$. Throughout, we consider p -values of ~ 0.005 and ≤ 0.001 to be marginal and significant evidence for the FRB-galaxy correlation, respectively.

⁴ FRBX: Tools for simulating, forecasting, and analyzing statistical cross-correlations between FRBs and other cosmological sources are available at <https://github.com/mrafieir/frbx>.

⁵ The variance $\text{Var}(\hat{\alpha}_{L,z})$ is estimated from the ensemble of mock FRB catalogs.

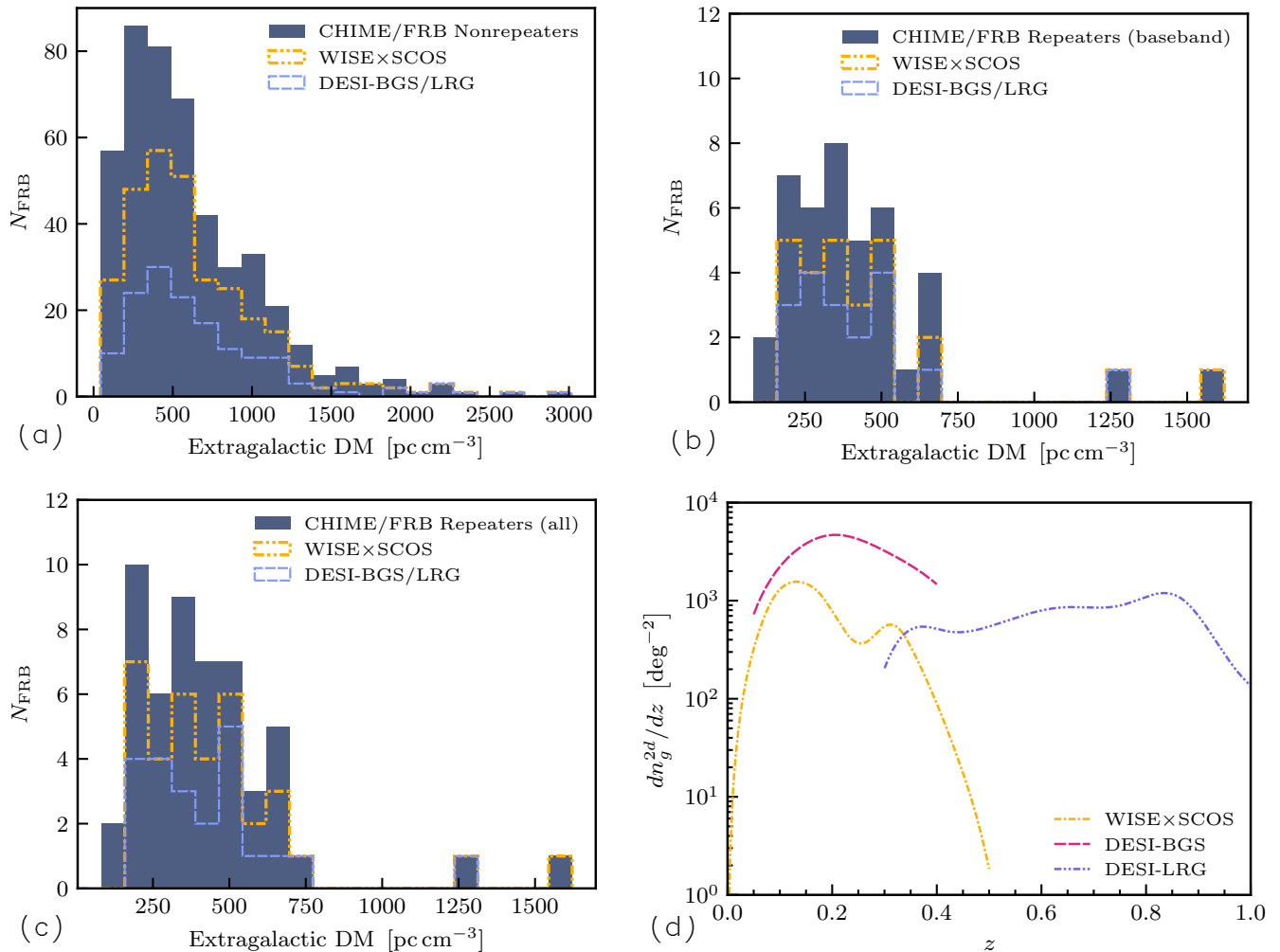


Figure 1. Panels (a)–(c): FRB DM distributions, including the subsets of FRBs that overlap with galaxy surveys for comparison. Panel (d): galaxy redshift distributions (see Table 1).

As described extensively by Rafiei-Ravandi et al. (2021), the angular cross power spectrum C_ℓ^{fg} and hence all its associated statistics, including the global p -values, can be computed for *binned* catalogs. For instance, in Section 4 of this work, we bin the repeaters (all) sample by median DM in order to pin down the DM dependence of a significant correlation with WISE×SCOS galaxies that are binned by redshift endpoints. In Appendix A of Rafiei-Ravandi et al. (2021), we showed that $L_{\text{max}} = 1396$ ($N_{\text{side}} = 2048$, $\ell_{\text{max}} = 2000$) is an appropriate choice for CHIME/FRB Catalog 1 with header localizations. Assuming that baseband localization errors are 10 times smaller than header localization errors, we extend the search over template scales out to $L_{\text{max}} = 13960$, corresponding to the angular scale $\theta = \pi/L_{\text{max}} = 0.77$ in this work.

4. RESULTS

In this section, we compare the repeating and nonrepeating FRB samples through their correlations with

galaxy catalogs. In addition, we report a significant correlation between a sample of repeaters and WISE×SCOS galaxies. We show that the correlation is dominated by a single FRB source. Finally, we reproduce results for CHIME/FRB Catalog 1 with the updated pipeline parameters in this work.

Figure 3 shows the FRB-galaxy cross power spectra for the repeaters and nonrepeaters. We find that deviations in bandpowers (averaged power spectra in nonoverlapping ℓ -bins) are either consistent with each other within 1σ (WISE×SCOS and DESI-LRG) or inconclusive (DESI-BGS) on scales of $\ell \sim 1000$, where CHIME/FRB Catalog 1 (along with the “nonrepeaters,” which make up the majority of the catalog) shows significant positive correlations with the same galaxy surveys (see Figure 7 of Rafiei-Ravandi et al. 2021). Focusing on the repeaters in panel (b) of Figure 3, we find a statistically significant positive correlation between “repeaters (all)” with $\text{DM} > 395 \text{ pc cm}^{-3}$ (median extra-

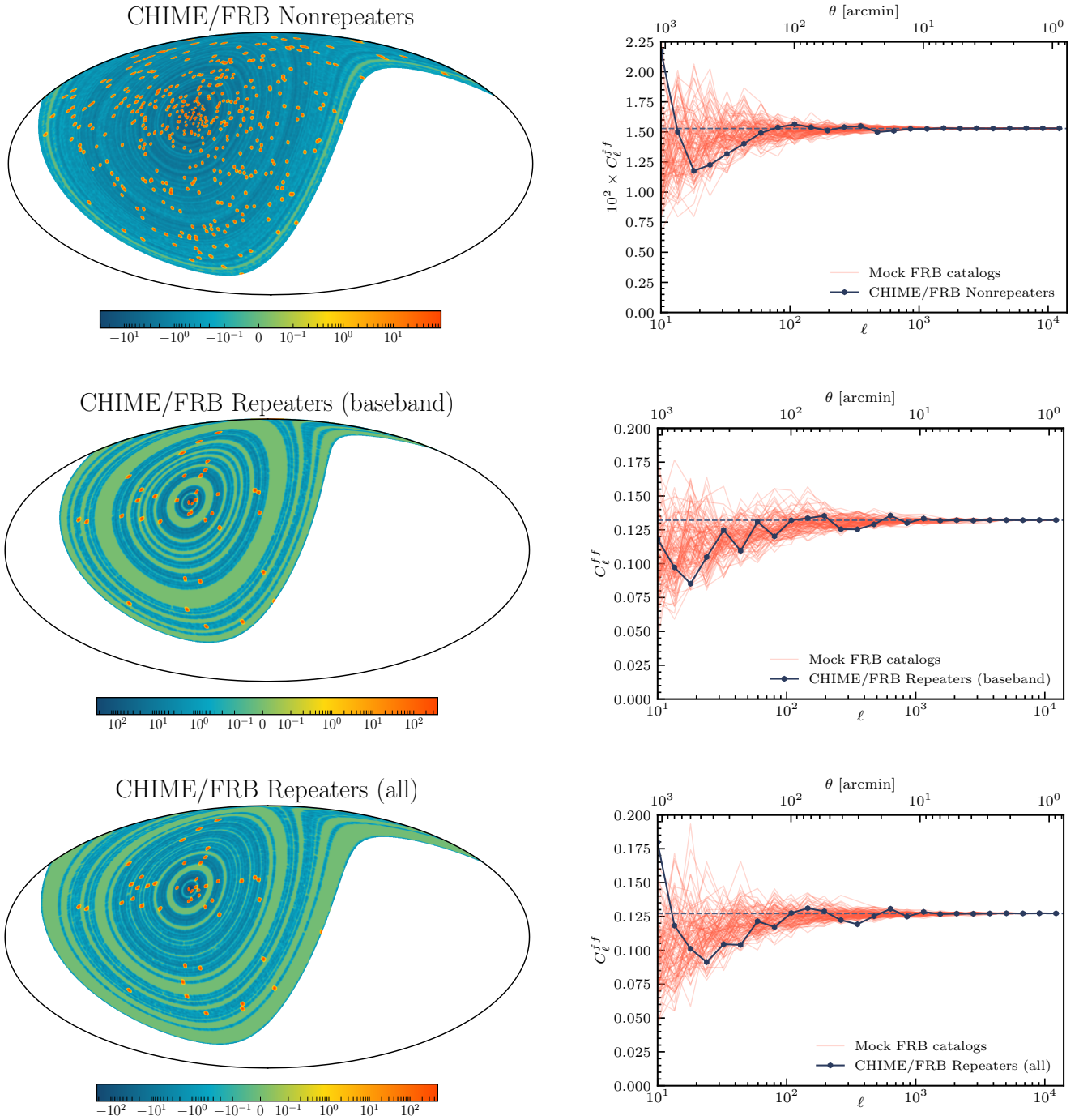


Figure 2. *Left column:* FRB overdensity maps, after incorporating random FRB catalogs, in Mollweide projection centered on Galactic longitude $l = 180^\circ$ in the Galactic coordinate system. Color bars indicate the full range of weighted density variations, including spurious fluctuations due to the survey geometry, which are modeled through “random” FRBs that encircle the north celestial pole (see Rafiei-Ravandi et al. 2021). Each FRB (orange point) contributes $1/(n_f^{2d}\Omega_{\text{pix}})$ to a pixel, where n_f^{2d} is the 2D number density and Ω_{pix} is the pixel area. *Right column:* angular auto power spectrum C_ℓ^{ff} for the three FRB samples on the left. Mock FRB catalogs (100 shown in each panel) trace the spatial distribution of real samples over a wide range of angular scales. Throughout, we assume Poisson-noise dominated FRB fields with $C_\ell^{ff} \approx 1/n_f^{2d}$ (dashed line) for template scales (L) corresponding to $315 \leq \ell \leq 13960$.

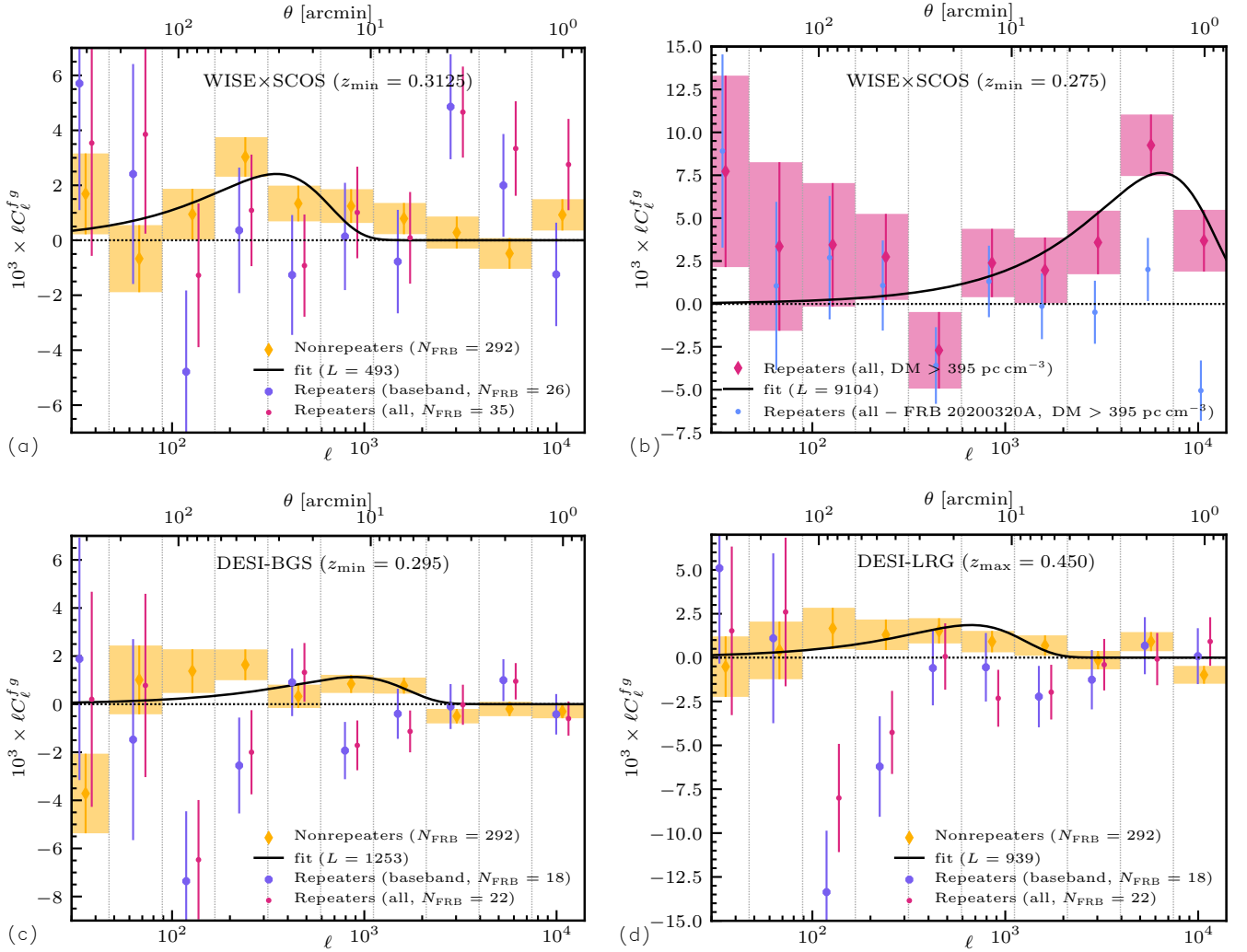


Figure 3. Angular cross power spectrum C_ℓ^{fg} for galaxy redshift bins (panels (a) through (d)) in which the “non-repeaters” correlation with galaxies are maximized. The displayed “fit” (solid black line) is the best-fit template of the form $C_\ell^{fg} = \alpha e^{-\ell^2/L^2}$ (fixed L) for the underlying cross power spectrum that is shown as shaded bandpowers. Error bars indicate 1σ deviations based on 1000 Monte Carlo realizations. Note the large error bars ($\propto N_{\text{FRB}}^{-1/2}$, assuming $C_\ell^{fg} \ll (C_\ell^{ff} C_\ell^{gg})^{1/2}$) for small FRB samples. In panel (b), the positive correlation between the DM-binned “repeaters (all)” sample and redshift-binned WISExSCOS galaxies is dominated by FRB 20200320A. In panel (d), the negative correlations are either marginal or totally insignificant after accounting for look-elsewhere factors (see Section 4).

galactic DM of the sample) and galaxies with redshift $z > 0.275$ in the WISExSCOS survey. The correlation has a local significance with $\text{SNR}_{\text{max}}^{(\text{data})} = 6.67$. After accounting for look-elsewhere factors, we obtain a global significance with a p -value < 0.001 (see Table 2) for this positive correlation. In other words, all the mock “repeaters (all)” catalogs with $\text{DM} > 395 \text{ pc cm}^{-3}$ correlate less significantly with WISExSCOS galaxies over the search space of template scales and minimum redshift endpoints.

Through visual inspection and pipeline reruns, we identify FRB 20200320A in the vicinity of four galaxies ($z \sim 0.3$) as the only source of this correlation (see Figure 4 and Table 3). FRB 20200320A is

a candidate (“silver”) repeater with a signal-to-noise ratio of 284.8 and observed inverse-variance-weighted average DM of $593.524(2) \text{ pc cm}^{-3}$ from the sample in CHIME/FRB Collaboration (2023). This candidate has two associated bursts that overlap within 1σ localization errors: FRB 20200320A (the first detection) and FRB 20201105A (the second burst with a signal-to-noise ratio of 9.3 and observed DM of $581.408(7) \text{ pc cm}^{-3}$). Taking into account the total number of bursts, DM, and sky location, CHIME/FRB Collaboration (2023) estimated a contamination rate of $R_{\text{cc}} = 0.92$ for this candidate repeater from the “silver” sample ($0.5 \leq R_{\text{cc}} < 5$); out of 25 “gold” and 14 “silver” sources, five are expected to be false pos-

Sample	Repeaters (baseband)	Repeaters (all)	Repeaters (all–FRB 20200320A)	Nonrepeaters	Catalog 1
WISE×SCOS	0.278 ($L=1853$, $z_{\min}=0.1375$)	0.007 ($L=9750$, $z_{\min}=0.275$)	...	< 0.001 ($L=493$, $z_{\min}=0.3125$)	< 0.001 ($L=613$, $z_{\min}=0.3125$)
WISE×SCOS ($z_{\min}=0.275$)	0.373 ($L=13960$, $DM < 395 \text{ pc cm}^{-3}$)	0.470 ($L=13960$, $DM < 395 \text{ pc cm}^{-3}$)	...	0.015 ($L=954$, $DM < 538 \text{ pc cm}^{-3}$)	0.012 ($L=989$, $DM < 535 \text{ pc cm}^{-3}$)
WISE×SCOS ($z_{\min}=0.275$)	0.463 ($L=5051$, $DM > 395 \text{ pc cm}^{-3}$)	< 0.001 ($L=9104$, $DM > 395 \text{ pc cm}^{-3}$)	0.757 ($L=5374$, $DM > 395 \text{ pc cm}^{-3}$)	0.012 ($L=349$, $DM > 538 \text{ pc cm}^{-3}$)	0.035 ($L=315$, $DM > 535 \text{ pc cm}^{-3}$)
DESI-BGS	0.204 ($L=13636$, $z_{\min}=0.050$)	0.291 ($L=9414$, $z_{\min}=0.050$)	...	0.006 ($L=1253$, $z_{\min}=0.295$)	0.001 ($L=1355$, $z_{\min}=0.295$)
DESI-LRG	0.545 ($L=1069$, $z_{\max}=0.712$)	0.506 ($L=950$, $z_{\max}=0.712$)	...	0.011 ($L=939$, $z_{\max}=0.45$)	0.001 ($L=1078$, $z_{\max}=0.485$)

Table 2. Statistical significance (p -value) of positive correlation between FRBs and galaxies after accounting for look-elsewhere factors in template scale (L) and redshift endpoint (z_{\min} or z_{\max}). Rows and columns correspond to galaxy and FRB samples, respectively. The L -values are characteristic scales for which p -values are presented. In the second and third rows, we select galaxies with the minimum redshift $z_{\min} = 0.275$ (significant correlation with the unbinned “repeaters (all)” sample) and bin the FRB samples by DM. The DM cuts are median values after accounting for galaxy survey footprints (see Section 2).

itive. Given the faint nature of the latter burst and the resulting uncertainty in its measured parameters, we consider derived properties of FRB 20200320A as primary throughout this analysis. The source of this candidate repeater was localized through the CHIME/FRB header localization pipeline (without baseband data) at right ascension $RA=42^{\circ}45_{-0.04}^{+0.02}$ (J2000) and declination $Dec=15^{\circ}84_{-0.06}^{+0.07}$ (J2000), which place the FRB outside the DESI-BGS/LRG survey footprint. The angular scale of the FRB-galaxy correlation is consistent with the FRB localization error $\theta_f \sim 1'$, corresponding to scales $\ell \sim 10^4$ beyond which C_{ℓ}^{fg} amplitude is suppressed substantially by the beam (Rafiei-Ravandi et al. 2020, 2021). We discuss this atypical yet robust result in Section 5.

Besides the positive correlation, we find for the first time statistical evidence for a negative correlation in the FRB-galaxy cross power spectrum. For instance, we examine panel (d) of Figure 3: the “repeaters (baseband)” sample correlates negatively with the DESI-BGS/LRG galaxies on scales $\ell \sim 100$. As a case in point, the negative bandpower centered on $\ell = 127.5$ has a local p -value (not accounting for look-elsewhere factors in ℓ or z) of

0.002 and < 0.001 for the DESI-BGS and DESI-LRG surveys, respectively. Computing a global significance through $\min_{L,z} \text{SNR}_{L,z}$ (see Section 3), we obtain the p -values 0.097 (DESI-BGS, $L = 768$, $z_{\min} = 0.24$) and 0.006 (DESI-LRG, $L = 315$, $z_{\max} = 0.45$), which fully account for the look-elsewhere effect.

We note that the locally significant negative correlation in the DESI-BGS case vanishes after accounting for look-elsewhere factors. In addition, negative correlations from the “repeaters (all)” sample are not statistically significant (p -values ~ 0.1) after accounting for the look-elsewhere effect. Thus, the only case that requires further consideration is the global p -value = 0.006 (DESI-LRG, $L = 315$, $z_{\max} = 0.45$). Furthermore, we note that repeaters and nonrepeaters differ by this negative correlation, which we discuss in the next section. Finally, we run the cross-correlation pipeline with the updated parameters $N_{\text{side}} = 8192$, $\ell_{\text{max}} = 14000$, and $315 \leq L \leq 13960$ for CHIME/FRB Catalog 1. We find that all the results presented in this work are consistent (i.e., no statistical or interpretational discrepancy after considering uncertainty limits throughout) with the work presented by Rafiei-Ravandi et al. (2021). In par-

#	WISE ID	RA (J2000)	Dec (J2000)	W1	W2	B	R	z
1	J024925.65+155711.3	42°3568758	15°9531491	14.49 ± 0.03	14.45 ± 0.07	20.8 ± 0.1	19.01 ± 0.07	0.470
2	J025000.22+154127.0	42°5009564	15°6908555	14.33 ± 0.03	14.14 ± 0.04	20.7 ± 0.1	18.82 ± 0.07	0.430
3	J024948.42+155059.7	42°4517860	15°8499300	14.57 ± 0.03	14.18 ± 0.04	20.35 ± 0.09	18.59 ± +0.07	0.310
4	J024947.67+155101.3	42°4486436	15°8503706	14.76 ± 0.03	14.43 ± 0.05	20.15 ± 0.08	18.46 ± 0.07	0.276
5	J024949.86+155102.4	42°4577628	15°8506816	14.62 ± 0.03	14.36 ± 0.05	20.8 ± 0.1	18.80 ± 0.07	0.367
6	J024950.98+155111.2	42°4624195	15°8531153	14.78 ± 0.03	14.44 ± 0.05	20.7 ± 0.1	18.74 ± 0.07	0.324
7	J025015.49+155056.4	42°5645709	15°8490154	14.78 ± 0.03	14.49 ± 0.05	20.03 ± 0.08	18.80 ± 0.07	0.279
8	J024929.63+154724.0	42°3734899	15°7900246	14.50 ± 0.03	14.28 ± 0.05	19.92 ± 0.07	18.35 ± 0.06	0.284
9	J024958.24+155535.5	42°4927080	15°9265453	14.40 ± 0.03	14.13 ± 0.04	19.90 ± 0.07	18.14 ± 0.06	0.287
10	J024928.10+155511.9	42°3671062	15°9199978	15.20 ± 0.04	15.05 ± 0.08	20.12 ± 0.08	19.14 ± 0.08	0.282

Table 3. WISE×SCOS galaxies in the vicinity ($< 10'$) of FRB 20200320A (#3–6, in bold, are $\lesssim 1'$ from the FRB; see Section 4). The photometric redshift “ z ” has an overall uncertainty of ≈ 0.033 . The WISE magnitudes “W1” ($3.4 \mu\text{m}$) and “W2” ($4.6 \mu\text{m}$) are in the Vega system, whereas the SCOS magnitudes “B” and “R” are in an AB system (see Bilicki et al. 2016).

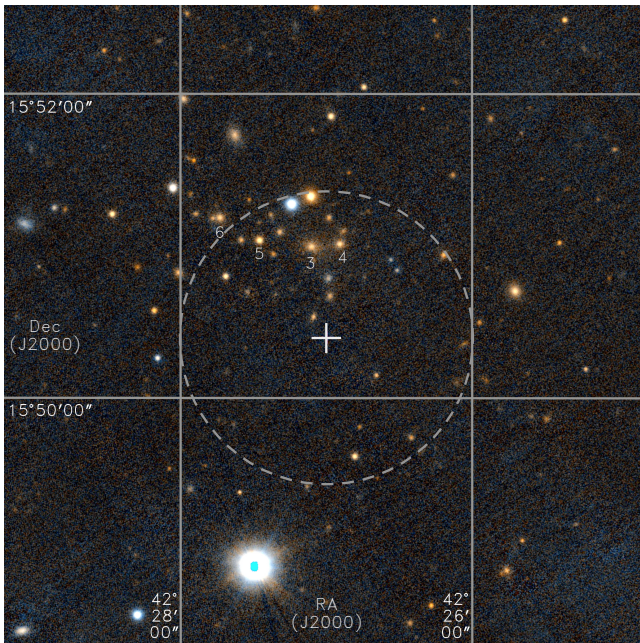


Figure 4. Pan-STARRS DR1 color image (Chambers et al. 2016; Baumann et al. 2022) of the vicinity of the candidate repeating FRB 20200320A. The dashed line encircles objects within $1'$ from the center, where the FRB is localized. Using the cross-correlation pipeline, we find a statistical association between the FRB and four WISE×SCOS galaxies, labeled #3–6 underneath each object, presumably all in the same dark matter halo at $z \approx 0.32$ (see Table 3).

ticular, we do not find any significant difference between results (p -values along with their corresponding template scale and redshift endpoint; see the two rightmost columns of Table 3) from nonrepeaters and Catalog 1.

5. DISCUSSION

In this article, we report on a statistically significant correlation (p -value < 0.001) between a sample of

CHIME/FRB repeaters and WISE×SCOS galaxies. We show that the correlation is dominated by the proximity of FRB 20200320A (extragalactic DM $\approx 550 \text{ pc cm}^{-3}$) to a group of four galaxies with mean redshift $z \approx 0.32$ (see Figure 4). In Table 3, we list all the galaxies from the WISE×SCOS survey in the vicinity of the FRB. The listed redshift values for the four galaxies mentioned above (galaxies #3–6) are consistent within 1.5σ ($\approx 130 h^{-1} \text{ Mpc}$) uncertainty, owing to photometric redshift errors. Hence, they could all be at the same redshift within the statistical uncertainty.

Assuming a Navarro–Frenk–White density profile (Navarro et al. 1997) and comoving units throughout, a dark matter halo with mass $M \sim 10^{12} M_{\odot}$, which is a typical value for galaxy groups with $\lesssim 4$ members (Tully 2015), spans a virial radius of $\sim 1'$ ($\sim 400 \text{ kpc}$) at this redshift on the sky. This picture is consistent with the FRB and galaxy group inhabiting the same dark matter halo. If we assume that galaxies #3–10 in Table 3 are members of the same gravitationally bound system, then we estimate the total halo mass to be $M \gtrsim 10^{14} M_{\odot}$. Nevertheless, no galaxy clusters have been identified near this sky location at redshift $z \approx 0.32$ (see the cluster catalog of Wen et al. 2018, which has a completeness limit of $\approx 50\%$ for clusters with mass $M \approx 10^{14} M_{\odot}$). Additionally, we do not find any Sunyaev-Zel’dovich or X-ray sources near this group of galaxies (Flesch 2016; Planck Collaboration et al. 2016; Salvato et al. 2018). More precise statements on this presumably bound system of galaxies would require spectroscopic redshifts, which were unavailable at the time of writing. Therefore, we defer the study of the galaxy group to future work.

If we assume that the FRB originated from redshift $z \approx 0.32$, then the mean IGM contribution to the observed DM is $\text{DM}_{\text{IGM}} \approx 325 \pm 180 \text{ pc cm}^{-3}$ (Macquart

et al. 2020; James et al. 2021). Computing the Galactic contribution based on two different models, we obtain $DM_{\text{gal}} = 38.92 \text{ pc cm}^{-3}$ (YMW16, Yao et al. 2017) and 45.53 pc cm^{-3} (NE2001, Cordes & Lazio 2002) with negligible uncertainties compared with the uncertainties in DM_{IGM} and DM_{halo} (see Section 1). Subtracting these contributions from the observed DM, we estimate the FRB host DM to be $DM_{\text{host}} \lesssim 380 \text{ pc cm}^{-3}$, which also includes any contributions from the host group/cluster electron profile. As pointed out by Ibik et al. (2023), most localized FRBs have $DM_{\text{host}} \lesssim 200 \text{ pc cm}^{-3}$, and the FRB host DM distribution, e.g., as a function of redshift, is largely unknown.

Based on the assumptions outlined earlier, we estimate the DM_{host} contribution from the host halo encompassing the galaxy group to be $DM_{\text{hh}} \gtrsim 70 \text{ pc cm}^{-3}$ (Connor & Ravi 2022). In the foreground, we identify the galaxy cluster NSC J024958+155217 (Northern Optical Cluster Survey III, Gal et al. 2009) at redshift $z \approx 0.12$ along the line of sight. This cluster has 12.0 ± 5.6 member galaxies that constitute a symmetric mass profile with a virial radius of $\approx 1 \text{ Mpc}$ (see Figure 5 of Gal et al. 2009). Assuming a halo mass of $\sim 10^{14} M_{\odot}$ with an “ICM” gas profile (Prochaska & Zheng 2019), we estimate that NSC J024958+155217 contributes $\gtrsim 100 \text{ pc cm}^{-3}$ to the DM_{IGM} of FRB 20200320A, which is localized to $\approx 3/2$ ($\approx 400 \text{ kpc}$) from the halo center. However, we highlight that the actual DM contribution from the host/intervening halo depends strongly on the uncertain distance between the FRB and the halo center (see, e.g., Figure 11 of Rafei-Ravandi et al. 2021).

We emphasize that FRB 20200320A is a “candidate” repeater comprised of two relatively different bursts (see Section 4), making this FRB-galaxy correlation intriguing. For instance, we note that a DM variation of $\approx 13.5 \text{ pc cm}^{-3}$ between the two FRBs, separated by 7.5 months, is large compared with observations of published repeaters that have typically shown smaller DM variations, e.g., from $< 0.15 \text{ pc cm}^{-3}$ in 10 months (Nimmo et al. 2023) to $\sim 4 \text{ pc cm}^{-3}$ in $\sim 1.5 - 3 \text{ yr}$ (Hilmarsson et al. 2021; Kumar et al. 2023). Here, the only other comparator is the “candidate” repeating FRB 20190107B (CHIME/FRB Collaboration 2023) with a DM variation of $\approx 14 \text{ pc cm}^{-3}$ in two months. Furthermore, FRB 20200320A has a scattering timescale of $2.46(3) \text{ ms}$ at 600 MHz (see Figure 13 of CHIME/FRB Collaboration 2023), $\lesssim 1\%$ of which could be produced by the Galactic ISM based on the NE2001 and YMW16 models. Given the FRB redshift, the remaining $\gtrsim 99\%$ of scattering could originate from the host CGM and circum-burst environment (Macquart & Koay 2013; Masui et al. 2015; Prochaska & Neeleman

2018; Chawla et al. 2022; Ocker et al. 2023; Sammons et al. 2023). In sharp contrast, FRB 20201105A (the second burst from presumably the same source) has a scattering timescale of $\ll 1 \text{ ms}$ at 600 MHz (CHIME/FRB Collaboration 2023). These burst-to-burst variations in DM and scattering further motivate follow-up observations of the FRB and galaxy group in order to identify and characterize the exact host through interferometry and spectroscopy at higher angular and frequency resolutions, respectively. With a burst rate of $3.91_{-3.78}^{+14.60} \times 10^{-2} \text{ hr}^{-1}$ (CHIME/FRB Collaboration 2023), any follow-up radio observations of the FRB (e.g., to verify whether the “candidate” is indeed a repeater with two bursts, or two nonrepeaters are associated with the same galaxy group/cluster) would be feasible only for continuous scans over $\sim \text{days-month}$. In the meantime, spectroscopy of the galaxy group could shed light on our understanding of potential environments that the FRB source might inhabit.

The association between FRB 20200320A and a galaxy group is not a typical result from statistical cross-correlations with large numbers of roughly localized sources; typically, we expect a large fraction of the sources to contribute statistically to any high-SNR detections (see, e.g., the results on nonrepeaters in Table 2). Nonetheless, this positive correlation is robust, since we use an appropriate template for the one-halo term and account for all look-elsewhere factors throughout the pipeline. This is the first time that a presumably bound system of galaxies has been discovered using FRB observations. Indeed, we would obtain the same result if we were to cross-match the FRB sample with a catalog of galaxy groups/clusters containing the group of four galaxies here. Therefore, we strongly suggest including catalogs of galaxy groups and clusters in direct host association pipelines even for FRBs with $\sim 1'$ localization precision.

In addition, we find evidence for a negative correlation between our “repeaters (baseband)” sample of FRBs and DESI-LRG galaxies. Negative FRB-galaxy correlations were formalized and forecast analytically by Rafei-Ravandi et al. (2020). The formalism was applied for the first time to real data (CHIME/FRB Catalog 1) by Rafei-Ravandi et al. (2021). In this work, we report the statistical significance of the negative correlation as $p\text{-value} = 0.006$ ($L = 315$, $z_{\text{max}} = 0.45$), which is interesting yet marginal. We do not find any such evidence for negative correlations in the analysis of “non-repeaters,” suggesting hypothetically that repeaters and nonrepeaters might cluster differently in dark matter halos over angular scales $\sim 0^{\circ}.5$. However, negative terms in the FRB-galaxy cross power spectrum C_{ℓ}^{fg} might

arise only from propagation effects due to intervening plasma (Rafiei-Ravandi et al. 2020). For instance, a negative DM-completeness term could stem from DM perturbations caused by electron anisotropy along the line of sight. These perturbations decrease the probability of detecting FRBs above a fixed signal-to-noise ratio threshold (i.e., increased DM: fluence preserved, signal-to-noise ratio reduced). In such a scenario, the observed number density of FRBs, apparently correlated with galaxies through foreground electrons, experiences a deficit due to the influence of DM perturbations. Consequently, this deficit results in the appearance of a negative contribution to C_ℓ^{fg} . Considering the borderline significance (99.4% CL, after accounting for the look-elsewhere effect in L and z_{\max}) of this negative correlation based on a relatively small sample size ($N_{\text{FRB}} = 18$), we defer any additional analysis regarding it, such as characterizing the instrumental selection function for the “repeaters (baseband)” sample, to future work.

Would we expect the repeaters to show an overall positive correlation with galaxies, in light of the results on nonrepeaters? This depends on the ℓ -dependence of the cross-correlations. The repeater population has larger C_ℓ^{fg} error bars (see Figure 3), so if the two FRB populations had the same ℓ -dependence, then we would not expect the repeaters to show a statistically significant cross-correlation. On the other hand, if the repeaters (ℓC_ℓ^{fg}) peaked at higher ℓ -values (compared to nonrepeaters), which is plausible because the repeaters have more precise localization, then we might find a cross-correlation at higher L -values. Before we did the analysis, either outcome was possible. However, the lack of an overall positive correlation between the repeating FRBs (excluding FRB 20200320A) and galaxies is unsurprising, given the small sample size. The CHIME/FRB baseband system is continuously localizing repeating and nonrepeating sources, enabling future explorations of the FRB phenomenon through cross-correlations with large-scale structure. The results in this work will improve with larger FRB catalogs in the future.

ACKNOWLEDGMENTS

We acknowledge that CHIME is located on the traditional, ancestral, and unceded territory of the Syilx/Okanagan people. We are grateful to the staff of the Dominion Radio Astrophysical Observatory, which is operated by the National Research Council of Canada. CHIME is funded by a grant from the Canada Foundation for Innovation (CFI) 2012 Leading Edge Fund (Project 31170) and by contributions from the provinces of British Columbia, Québec, and Ontario. The CHIME/FRB Project is funded by a grant from the CFI 2015 Innovation Fund (Project 33213) and by contributions from the provinces of British Columbia and Québec, and by the Dunlap Institute for Astronomy and Astrophysics at the University of Toronto. Additional support was provided by the Canadian Institute for Advanced Research (CIFAR), McGill University and the McGill Space Institute thanks to the Trottier Family Foundation, and the University of British Columbia. Research at Perimeter Institute is supported by the Government of Canada through Industry Canada and by the Province of Ontario through the Ministry of Research & Innovation. The Dunlap Institute is funded through an endowment established by the David Dunlap family and the University of Toronto.

K. M. S. was supported by an NSERC Discovery Grant and a CIFAR fellowship. Z. P. is a Dunlap Fellow. M. B. is a McWilliams fellow and an IAU Gruber fellow. M. D. is supported by a CRC Chair, NSERC Discovery Grant, CIFAR, and by the FRQNT Centre de Recherche en Astrophysique du Québec (CRAQ). G. M. E. is supported by an NSERC Discovery Grant (RGPIN-2020-0455), and by a Canadian Statistical Sciences Institute Collaborative Research Team grant. B. M. G. is supported by an NSERC Discovery Grant (RGPIN-2022-03163), and by the Canada Research Chairs (CRC) program. V. M. K. holds the Lorne Trottier Chair in Astrophysics & Cosmology, a Distinguished James McGill Professorship, and receives support from an NSERC Discovery grant (RGPIN 228738-13), from an R. Howard Webster Foundation Fellowship from CIFAR, and from the FRQNT CRAQ. C. L. is a NASA Hubble Fellowship Program (NHFP) Einstein Fellow, supported by NASA through the NASA Hubble Fellowship grant #HST-HF2-51536.001-A awarded by the Space Telescope Science Institute, which is operated by the Association of Universities for Research in Astronomy, Incorporated, under NASA contract NAS5-26555. K. W. M. holds the Adam J. Burgasser Chair in Astrophysics and is supported by NSF grants (2008031, 2018490). A. P. is funded by the NSERC Canada Graduate Scholarships –

Doctoral program. A. B. P. is a Banting Fellow, a McGill Space Institute (MSI) Fellow, and a Fonds de Recherche du Québec – Nature et Technologies (FRQNT) postdoctoral fellow. D. C. S. is supported by an NSERC Discovery Grant (RGPIN-2021-03985) and by a Canadian Statistical Sciences Institute (CANSSI) Collaborative Research Team Grant. This research was enabled in part by support provided by WestGrid (www.westgrid.ca) and Compute Canada (www.computeCanada.ca). The Photometric Redshifts for the Legacy Surveys (PRLS) catalog used in this article was produced thanks to funding from the U.S. Department of Energy Office of Science, Office of High Energy Physics via grant DE-SC0007914. This research has made use of “Aladin sky atlas” developed at CDS, Strasbourg Observatory, France. The Pan-STARRS1 Surveys (PS1) and the PS1 public science archive have been made possible through

contributions by the Institute for Astronomy, the University of Hawaii, the Pan-STARRS Project Office, the Max-Planck Society and its participating institutes, the Max Planck Institute for Astronomy, Heidelberg, and the Max Planck Institute for Extraterrestrial Physics, Garching, The Johns Hopkins University, Durham University, the University of Edinburgh, the Queen’s University Belfast, the Harvard-Smithsonian Center for Astrophysics, the Las Cumbres Observatory Global Telescope Network Incorporated, the National Central University of Taiwan, the Space Telescope Science Institute, the National Aeronautics and Space Administration under grant No. NNX08AR22G issued through the Planetary Science Division of the NASA Science Mission Directorate, the National Science Foundation grant No. AST-1238877, the University of Maryland, Eotvos Lorand University (ELTE), the Los Alamos National Laboratory, and the Gordon and Betty Moore Foundation.

REFERENCES

- Aghanim, N., Akrami, Y., Ashdown, M., et al. 2020, *Astronomy & Astrophysics*, 641, A6, doi: [10.1051/0004-6361/201833910](https://doi.org/10.1051/0004-6361/201833910)
- Bannister, K. W., Deller, A. T., Phillips, C., et al. 2019, *Science*, 365, 565, doi: [10.1126/science.aaw5903](https://doi.org/10.1126/science.aaw5903)
- Baumann, M., Boch, T., Pineau, F.-X., et al. 2022, in *Astronomical Society of the Pacific Conference Series*, Vol. 532, *Astronomical Society of the Pacific Conference Series*, ed. J. E. Ruiz, F. Pierfederci, & P. Teuben, 7
- Bhandari, S., Sadler, E. M., Prochaska, J. X., et al. 2020, *The Astrophysical Journal Letters*, 895, L37, doi: [10.3847/2041-8213/ab672e](https://doi.org/10.3847/2041-8213/ab672e)
- Bhandari, S., Heintz, K. E., Aggarwal, K., et al. 2022, *The Astronomical Journal*, 163, 69, doi: [10.3847/1538-3881/ac3aec](https://doi.org/10.3847/1538-3881/ac3aec)
- Bhandari, S., Gordon, A. C., Scott, D. R., et al. 2023, *The Astrophysical Journal*, 948, 67, doi: [10.3847/1538-4357/acc178](https://doi.org/10.3847/1538-4357/acc178)
- Bhardwaj, M., Kirichenko, A. Y., Michilli, D., et al. 2021a, *The Astrophysical Journal Letters*, 919, L24, doi: [10.3847/2041-8213/ac223b](https://doi.org/10.3847/2041-8213/ac223b)
- Bhardwaj, M., Gaensler, B. M., Kaspi, V. M., et al. 2021b, *The Astrophysical Journal*, 910, L18, doi: [10.3847/2041-8213/abeaa6](https://doi.org/10.3847/2041-8213/abeaa6)
- Bilicki, M., Peacock, J. A., Jarrett, T. H., et al. 2016, *The Astrophysical Journal Supplement Series*, 225, 5, doi: [10.3847/0067-0049/225/1/5](https://doi.org/10.3847/0067-0049/225/1/5)
- Chambers, K. C., Magnier, E. A., Metcalfe, N., et al. 2016, arXiv e-prints, arXiv:1612.05560, doi: [10.48550/arXiv.1612.05560](https://doi.org/10.48550/arXiv.1612.05560)
- Chatterjee, S., Law, C. J., Wharton, R. S., et al. 2017, *Nature*, 541, 58, doi: [10.1038/nature20797](https://doi.org/10.1038/nature20797)
- Chawla, P., Kaspi, V. M., Ransom, S. M., et al. 2022, *The Astrophysical Journal*, 927, 35, doi: [10.3847/1538-4357/ac49e1](https://doi.org/10.3847/1538-4357/ac49e1)
- CHIME Collaboration. 2022, *The Astrophysical Journal Supplement Series*, 261, 29, doi: [10.3847/1538-4365/ac6fd9](https://doi.org/10.3847/1538-4365/ac6fd9)
- CHIME/FRB Collaboration. 2018, *The Astrophysical Journal*, 863, 48, doi: [10.3847/1538-4357/aad188](https://doi.org/10.3847/1538-4357/aad188)
- . 2019a, *Nature*, 566, 235, doi: [10.1038/s41586-018-0864-x](https://doi.org/10.1038/s41586-018-0864-x)
- . 2019b, *The Astrophysical Journal Letters*, 885, L24, doi: [10.3847/2041-8213/ab4a80](https://doi.org/10.3847/2041-8213/ab4a80)
- . 2021, *The Astrophysical Journal Supplement Series*, 257, 59, doi: [10.3847/1538-4365/ac33ab](https://doi.org/10.3847/1538-4365/ac33ab)
- . 2023, arXiv e-prints, arXiv:2301.08762, doi: [10.48550/arXiv.2301.08762](https://doi.org/10.48550/arXiv.2301.08762)
- Connor, L., & Ravi, V. 2022, *Nature Astronomy*, 6, 1035, doi: [10.1038/s41550-022-01719-7](https://doi.org/10.1038/s41550-022-01719-7)
- Connor, L., Ravi, V., Catha, M., et al. 2023, arXiv e-prints, arXiv:2302.14788, doi: [10.48550/arXiv.2302.14788](https://doi.org/10.48550/arXiv.2302.14788)
- Cook, A. M., Bhardwaj, M., Gaensler, B. M., et al. 2023, *The Astrophysical Journal*, 946, 58, doi: [10.3847/1538-4357/acbbd0](https://doi.org/10.3847/1538-4357/acbbd0)
- Cordes, J. M., & Lazio, T. J. W. 2002, arXiv e-prints, astro. <https://ui.adsabs.harvard.edu/abs/2002astro.ph..7156C>
- Eftekhari, T., & Berger, E. 2017, *The Astrophysical Journal*, 849, 162, doi: [10.3847/1538-4357/aa90b9](https://doi.org/10.3847/1538-4357/aa90b9)
- Flesch, E. W. 2016, *Publications of the Astronomical Society of Australia*, 33, e052, doi: [10.1017/pasa.2016.44](https://doi.org/10.1017/pasa.2016.44)

- Fonseca, E., Andersen, B. C., Bhardwaj, M., et al. 2020, *The Astrophysical Journal Letters*, 891, L6, doi: [10.3847/2041-8213/ab7208](https://doi.org/10.3847/2041-8213/ab7208)
- Gal, R. R., Lopes, P. A. A., de Carvalho, R. R., et al. 2009, *The Astronomical Journal*, 137, 2981, doi: [10.1088/0004-6256/137/2/2981](https://doi.org/10.1088/0004-6256/137/2/2981)
- Gordon, A. C., Fong, W.-f., Kilpatrick, C. D., et al. 2023, arXiv e-prints, arXiv:2302.05465, doi: [10.48550/arXiv.2302.05465](https://doi.org/10.48550/arXiv.2302.05465)
- Górski, K. M., Hivon, E., Banday, A. J., et al. 2005, *The Astrophysical Journal*, 622, 759, doi: [10.1086/427976](https://doi.org/10.1086/427976)
- Heintz, K. E., Prochaska, J. X., Simha, S., et al. 2020, *The Astrophysical Journal*, 903, 152, doi: [10.3847/1538-4357/abb6fb](https://doi.org/10.3847/1538-4357/abb6fb)
- Hilmarsson, G. H., Michilli, D., Spitler, L. G., et al. 2021, *The Astrophysical Journal*, 908, L10, doi: [10.3847/2041-8213/abdec0](https://doi.org/10.3847/2041-8213/abdec0)
- Ibik, A. L., Drout, M. R., Gaensler, B. M., et al. 2023, arXiv e-prints, arXiv:2304.02638, doi: [10.48550/arXiv.2304.02638](https://doi.org/10.48550/arXiv.2304.02638)
- James, C. W., Prochaska, J. X., Macquart, J. P., et al. 2021, arXiv e-prints, arXiv:2101.08005, <https://ui.adsabs.harvard.edu/abs/2021arXiv210108005J>
- Josephy, A., Chawla, P., Curtin, A. P., et al. 2021, arXiv e-prints, arXiv:2106.04353, <https://ui.adsabs.harvard.edu/abs/2021arXiv210604353J>
- Kourkchi, E., & Tully, R. B. 2017, *The Astrophysical Journal*, 843, 16, doi: [10.3847/1538-4357/aa76db](https://doi.org/10.3847/1538-4357/aa76db)
- Krakovski, T., Malek, K., Bilicki, M., et al. 2016, *A&A*, 596, <https://doi.org/10.1051/0004-6361/201629165>
- Kumar, P., Luo, R., Price, D. C., et al. 2023, arXiv e-prints, arXiv:2304.01763, doi: [10.48550/arXiv.2304.01763](https://doi.org/10.48550/arXiv.2304.01763)
- Law, C. J., Butler, B. J., Prochaska, J. X., et al. 2020, *The Astrophysical Journal*, 899, 161, doi: [10.3847/1538-4357/aba4ac](https://doi.org/10.3847/1538-4357/aba4ac)
- Law, C. J., Sharma, K., Ravi, V., et al. 2023, arXiv e-prints, arXiv:2307.03344, doi: [10.48550/arXiv.2307.03344](https://doi.org/10.48550/arXiv.2307.03344)
- Lorimer, D. R., Bailes, M., McLaughlin, M. A., Narkevic, D. J., & Crawford, F. 2007, *Science*, 318, 777, doi: [10.1126/science.1147532](https://doi.org/10.1126/science.1147532)
- Macquart, J.-P., & Koay, J. Y. 2013, *The Astrophysical Journal*, 776, 125, doi: [10.1088/0004-637X/776/2/125](https://doi.org/10.1088/0004-637X/776/2/125)
- Macquart, J. P., Prochaska, J. X., McQuinn, M., et al. 2020, *Nature*, 581, 391, doi: [10.1038/s41586-020-2300-2](https://doi.org/10.1038/s41586-020-2300-2)
- Marcote, B., Nimmo, K., Hessels, J. W. T., et al. 2020, *Nature*, 577, 190, doi: [10.1038/s41586-019-1866-z](https://doi.org/10.1038/s41586-019-1866-z)
- Masui, K., Lin, H.-H., Sievers, J., et al. 2015, *Nature*, 528, 523, doi: [10.1038/nature15769](https://doi.org/10.1038/nature15769)
- Michilli, D., Masui, K. W., Mckinven, R., et al. 2021, *The Astrophysical Journal*, 910, 147, doi: [10.3847/1538-4357/abe626](https://doi.org/10.3847/1538-4357/abe626)
- Michilli, D., Bhardwaj, M., Brar, C., et al. 2023, *The Astrophysical Journal*, 950, 134, doi: [10.3847/1538-4357/accf89](https://doi.org/10.3847/1538-4357/accf89)
- Navarro, J. F., Frenk, C. S., & White, S. D. M. 1997, *Astrophys. J.*, 490, 493, doi: [10.1086/304888](https://doi.org/10.1086/304888)
- Nimmo, K., Hessels, J. W. T., Snelders, M. P., et al. 2023, *Monthly Notices of the Royal Astronomical Society*, 520, 2281, doi: [10.1093/mnras/stad269](https://doi.org/10.1093/mnras/stad269)
- Ocker, S. K., Cordes, J. M., Chatterjee, S., et al. 2023, *Monthly Notices of the Royal Astronomical Society*, 519, 821, doi: [10.1093/mnras/stac3547](https://doi.org/10.1093/mnras/stac3547)
- Petroff, E., Hessels, J. W. T., & Lorimer, D. R. 2022, *Astronomy and Astrophysics Review*, 30, 2, doi: [10.1007/s00159-022-00139-w](https://doi.org/10.1007/s00159-022-00139-w)
- Planck Collaboration, Ade, P. A. R., Aghanim, N., et al. 2016, *A&A*, 594, <https://doi.org/10.1051/0004-6361/201525823>
- Pleunis, Z., Good, D. C., Kaspi, V. M., et al. 2021, arXiv e-prints, arXiv:2106.04356, <https://ui.adsabs.harvard.edu/abs/2021arXiv210604356P>
- Prochaska, J. X., & Neeleman, M. 2018, *Monthly Notices of the Royal Astronomical Society*, 474, 318, doi: [10.1093/mnras/stx2824](https://doi.org/10.1093/mnras/stx2824)
- Prochaska, J. X., & Zheng, Y. 2019, *Monthly Notices of the Royal Astronomical Society*, 485, 648, doi: [10.1093/mnras/stz261](https://doi.org/10.1093/mnras/stz261)
- Rafiei-Ravandi, M. 2023, *FRBX*, Zenodo, doi: [10.5281/ZENODO.8409302](https://doi.org/10.5281/ZENODO.8409302)
- Rafiei-Ravandi, M., Smith, K. M., & Masui, K. W. 2020, *Physical Review D*, 102, 023528, doi: [10.1103/PhysRevD.102.023528](https://doi.org/10.1103/PhysRevD.102.023528)
- Rafiei-Ravandi, M., Smith, K. M., Li, D., et al. 2021, *The Astrophysical Journal*, 922, 42, doi: [10.3847/1538-4357/ac1dab](https://doi.org/10.3847/1538-4357/ac1dab)
- Ravi, V., Catha, M., D'Addario, L., et al. 2019, *Nature*, 572, 352, doi: [10.1038/s41586-019-1389-7](https://doi.org/10.1038/s41586-019-1389-7)
- Ravi, V., Catha, M., Chen, G., et al. 2023, arXiv e-prints, arXiv:2301.01000, doi: [10.48550/arXiv.2301.01000](https://doi.org/10.48550/arXiv.2301.01000)
- Ruiz-Macias, O., Zarrouk, P., Cole, S., et al. 2020, *Research Notes of the American Astronomical Society*, 4, 187, doi: [10.3847/2515-5172/abc25a](https://doi.org/10.3847/2515-5172/abc25a)
- Salvato, M., Buchner, J., Budavári, T., et al. 2018, *Monthly Notices of the Royal Astronomical Society*, 473, 4937, doi: [10.1093/mnras/stx2651](https://doi.org/10.1093/mnras/stx2651)
- Sammons, M. W., Deller, A. T., Glowacki, M., et al. 2023, arXiv e-prints, arXiv:2305.11477, doi: [10.48550/arXiv.2305.11477](https://doi.org/10.48550/arXiv.2305.11477)

- Sharma, K., Somalwar, J., Law, C., et al. 2023, *The Astrophysical Journal*, 950, 175, doi: [10.3847/1538-4357/accf1d](https://doi.org/10.3847/1538-4357/accf1d)
- Tully, R. B. 2015, *The Astronomical Journal*, 149, 171, doi: [10.1088/0004-6256/149/5/171](https://doi.org/10.1088/0004-6256/149/5/171)
- Wen, Z. L., Han, J. L., & Yang, F. 2018, *Monthly Notices of the Royal Astronomical Society*, 475, 343, doi: [10.1093/mnras/stx3189](https://doi.org/10.1093/mnras/stx3189)
- Yang, X., Xu, H., He, M., et al. 2021, *The Astrophysical Journal*, 909, 143, doi: [10.3847/1538-4357/abddb2](https://doi.org/10.3847/1538-4357/abddb2)
- Yao, J. M., Manchester, R. N., & Wang, N. 2017, *The Astrophysical Journal*, 835, 29, doi: [10.3847/1538-4357/835/1/29](https://doi.org/10.3847/1538-4357/835/1/29)
- Zhou, R., Newman, J. A., Mao, Y.-Y., et al. 2020a, *Monthly Notices of the Royal Astronomical Society*, doi: [10.1093/mnras/staa3764](https://doi.org/10.1093/mnras/staa3764)
- Zhou, R., Newman, J. A., Dawson, K. S., et al. 2020b, *Research Notes of the American Astronomical Society*, 4, 181, doi: [10.3847/2515-5172/abc0f4](https://doi.org/10.3847/2515-5172/abc0f4)